



Original Article

High-Resolution Measurements of Leakage Flow Inside the Hinge of a Large-scale Bileaflet Mechanical Heart Valve Hinge Model

EWA KLUSAK and NATHAN J. QUINLAN

Mechanical Engineering, National University of Ireland Galway, Galway, Ireland

(Received 13 November 2018; accepted 13 June 2019; published online 24 June 2019)

Associate Editor Ajit P. Yoganathan oversaw the review of this article.

Abstract

Purpose—It is believed that non-physiological leakage flow through hinge gaps during diastole contributes to thrombus formation in Bileaflet Mechanical Heart Valves (BMHVs). Because of the small scale and difficulty of experimental access, fluid dynamics inside the hinge cavity has not yet been characterised in detail. The objective is to investigate small-scale structure inside the hinge experimentally, and gain insight into its role in stimulating cellular responses.

Methods—An optically accessible scaled-up model of a BMHV hinge was designed and built, preserving dynamic similarity to a clinical BMHV. Particle Image Velocimetry (PIV) was used to visualize and quantify the flow fields inside the hinge at physiological Reynolds number and dimensionless pressure drop. The flow was measured at in-plane and out-of-plane spatial resolution of 32 and 86 μm , respectively, and temporal resolution of 297 μs . **Results**—Likely flow separation on the ventricular surface of the cavity has been observed for the first time, and is a source of unsteadiness and perhaps turbulence. The shear stress found in all planes exceeds the threshold of platelet activation, ranging up to 168 Pa.

Conclusions—The scale-up approach provided new insight into the nature of the hinge flow and enhanced understanding of its complexity. This study revealed flow features that may induce blood element damage.

Keywords—Mechanical heart valve, Particle image velocimetry, Hinge flow, Heart valve thrombosis, Hemodynamics, Shear stress, Fluid dynamics.

INTRODUCTION

Mechanical heart valves (MHVs) are an established treatment option for patients requiring heart valve replacement. MHVs evolved into multiple designs of which the bileaflet mechanical heart valve (BMHV) remains the most common choice.^{9,13,18,49} BMHVs have proven their durability over bioprostheses.^{20,39} However, they are associated with adverse post-procedural clinical events such as thrombosis, thromboembolism or haemolysis. To decrease the risk of complications related to blood clot formation in the circulatory system, life-long anticoagulation therapy is needed.^{3,7,9,20,25,39} Anticoagulant intake however is not an ultimate solution, as an increased risk of anticoagulation-related hemorrhage (uncontrolled bleeding) has been previously observed in patients with MHVs.^{11,31}

BMHV thrombogenicity varies between designs and has been attributed to non-physiological fluid dynamics.^{11,31} Previous studies showed that the blood damage may occur at various phases of the flow through the BMHVs. In particular, leaflet closure and leakage flow through the hinges of BMHV have been shown to play a significant role in blood damage.^{15–17,22,23,28,41} Studies of BMHV explants confirmed that the hinge cavity is a favourable location for thrombus attachment and growth.^{10,42} Early experimental studies confirmed that leakage flow on the ventricular side of the hinge results in elevated shear stress, flow separation, stagnation and recirculation, introducing non-physiological loading of blood elements which may lead to red blood cell damage, platelet activation, and platelet aggregation.^{15–17,22,41,44,48} Turbulence in blood flow is known to cause elevated levels of blood damage.^{6,24,40,46}

Address correspondence to Nathan J. Quinlan, Mechanical Engineering, National University of Ireland Galway, Galway, Ireland. Electronic mail: nathan.quinlan@nuigalway.ie

Experimental measurement of flow in and near the hinge is challenging because of the small scale of the hinge structure and limited optical access. Previous researchers have quantified jet flow issuing from the hinge of a closed valve. Strong velocity fluctuations, which may indicate turbulence, have been observed.^{26,40} Ellis *et al.*¹⁶ and Jun *et al.*²³ employed Laser Doppler Velocimetry (LDV) and microPIV respectively to measure velocity inside transparent models of BMHV hinges. However, whole-field instantaneous measurements were not possible in the aforementioned studies, as both LDV and microPIV techniques have their limitations. Simon *et al.*³⁶ and Yun *et al.*⁴⁷ conducted computational modelling of flow inside the hinge with Navier-Stokes and Lattice-Boltzmann approaches respectively. Models like these provide highly resolved flow fields, but require experimental validation.

High spatial measurement resolution is important not only because of the small scale of the hinge, but also to reveal small-scale flow structures that may be present in and near the hinge. Simon *et al.*³⁶ estimated a Reynolds number of 150 in the hinge gap, suggesting laminar flow. However, the geometry is complex, and the leakage jet flow on the ventricular side of the hinge has been reported to be unsteady.^{26,45} Turbulent or unsteady flow in the hinges has not been ruled out by experimental evidence. Since the role of turbulence in blood damage is still poorly quantified, it is important to measure the flow field directly at small scales.³² This requires high spatial resolution. Unsteady, transitional or turbulent flow, if present, also entails rapidly fluctuating unsteady flow, calling for high temporal resolution in measurements. High-resolution measurement of flow inside the hinge cavity may also provide insight into the generation of the leakage jets.

The objective of this study is to obtain comprehensive knowledge of the fluid dynamics inside the BMHV hinge cavity to enhance understanding of its role in blood damage, by performing experimental velocity field measurements at extremely high spatial and temporal resolution. In particular, we aim to characterise unsteady structures (if any) of the flow and quantify viscous shear stresses as a measure of the mechanical loading experienced by blood elements. High resolution is achieved by conducting PIV measurements in a large-scale transparent model of the hinge region of a BMHV. Moreover, this study investigates the impact of measurement spatial and temporal resolution on results. This work is a continuation of a previous study by Klusak *et al.*,²⁶ where flow downstream of the hinge was investigated. Methods and test rig remain unchanged. However, a new improved model with transparent hinge cavities, based on μ -CT scans of a clinical BMHV, is incorporated to enable in-hinge flow investigation.

MATERIALS AND METHODS

Scaled-Up Hinge Model

A scaled-up model of the hinge region has been built to enhance spatial and temporal resolution of flow measurements inside the hinge cavity. The model is based on μ -CT scans of a clinically available St. Jude Medical (SJM) BMHV, scaled geometrically by a factor of 11.6. The experiment is designed in accordance with dimensional analysis to preserve the dimensionless transvalvular pressure drop

$$\Delta p^* = \frac{\Delta p}{\left(\frac{1}{2} \frac{\rho^2}{\rho D^2}\right)} \quad (1)$$

between the clinical and scaled-up valves, where Δp denotes the transvalvular pressure drop, μ is dynamic viscosity, ρ is density, and D is valve diameter. Consequently, the local Reynolds number is preserved. This ensures that the correct flow physics are replicated. The dimensional analysis and scaling design have been described in detail by Bellofiore *et al.*⁴ and Klusak *et al.*²⁶

As shown in Fig. 1, the model consists of a hinge base, two butterfly recesses and a portion of each of two leaflets with their hinge protrusion. The hinge base and two butterfly recesses were vacuum-formed (Enform Plastics Ltd., Ennis, Ireland) from transparent, 400 μ m-thick polyethylene terephthalate (PET), for optical access to the hinge recess. The hinge model is resting on a supporting plate. The model is installed in a cylindrical tubular test section, with the hinge flat level on the tube mid-plane. There is no flow in the test section below the hinge base; all flow passes through the hinges (Fig. 1).

The tube is transparent, with an inner diameter of 140 mm and wall thickness of 5 mm. In the model, the housing and leaflet are separated by a uniform gap width of 150 μ m (in equivalent physiological scale, 1.74 mm in model scale) as shown in Fig. 1. The choice of the gap width follows previous work presented by Klusak *et al.*²⁶ Moreover, the gap width of 150 μ m falls into the range of the gap width measured in the reconstructed valve geometry from μ -CT scans. The tube and the leaflets were manufactured by Riteway Engineering Ltd. (Galway, Ireland) from transparent PMMA to allow optical access to the measurement section.

Experimental Apparatus

The model hinges are inserted into the large-scale heart valve flow simulator (Fig. 2), previously described by Bellofiore *et al.*^{4,5} and Klusak *et al.*²⁶ In brief, the test section consists of a transparent cylindrical tube housing the model hinges (Fig. 1c). In this study, blood is modelled as a Newtonian fluid, following the widespread approach

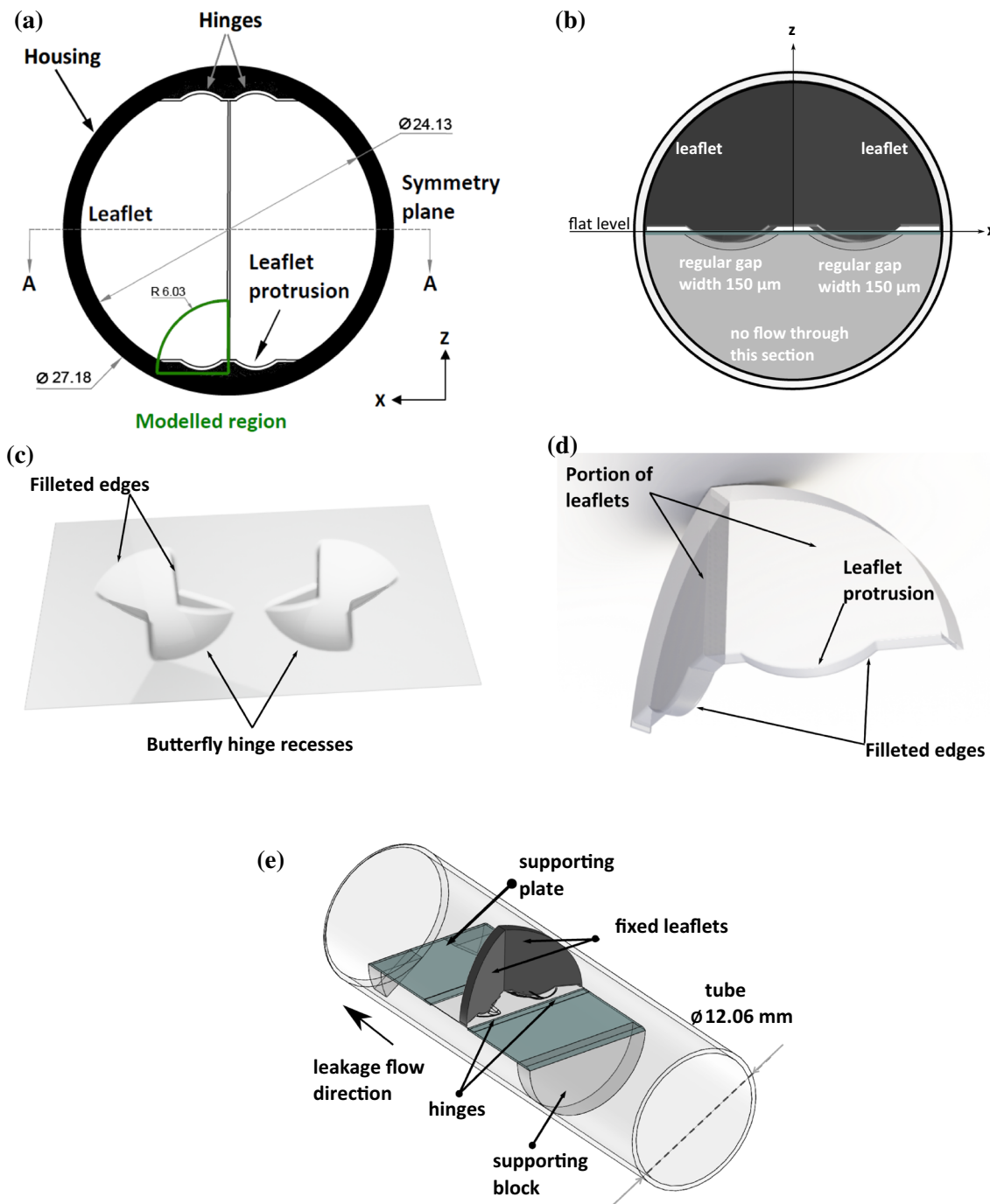


FIGURE 1. The BMHV hinge region model. (a) Modelled portion of the valve; (b) front view of two hinges model with constant, identical hinge gap width; (c) transparent hinge base and hinge recesses; (d) transparent leaflets; (e) test section with model enclosed in the transparent tube. All dimensions are presented in physiological scale.

in the literature (for example, Ellis,¹⁴ Simon,³⁸ and Manning²⁸). The test section is enclosed in a transparent square-section box, filled with water to minimise optical distortion. Although there is a significant refractive index mismatch between the fluid (water, 1.33) and the walls (1.49), we have previously found that this is mitigated by the small ratio of tube wall thickness (5 mm) to radius of

curvature (70 mm). PIV measurements in this experiment were conducted within the central 76.6% of the tube's diameter. Error that may arise from refractive index mismatch has been previously shown by Bellofiore *et al.*⁴ to be negligible compared to RMS error, as long as measurements are conducted within the central 79% of the tube in this configuration.

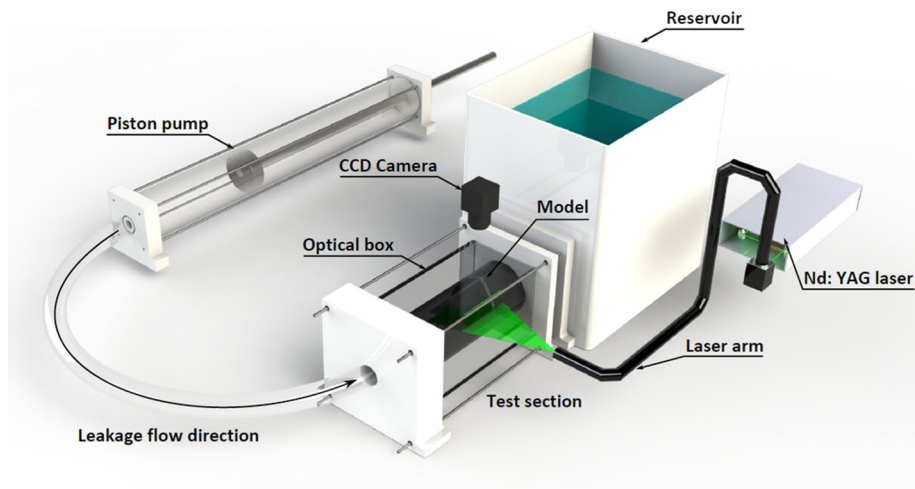


FIGURE 2. Scaled-up heart valve flow simulator rig with hinge model in the test section.

Measurement Locations and Test Conditions

The flow field was measured inside the hinge cavity as shown in Fig. 3a. Measurements were taken inside the hinge at eight planes below the flat level at $-86 \mu\text{m}$, -172 , -258 , -344 , -430 , -502 , -516 and $-588 \mu\text{m}$, as shown in Fig. 3b. These dimensions are expressed in equivalent physiological scale (i.e. scaled down by a factor of 11.6 with respect to the dimensions of the *in vitro* model).

Reverse leakage flow was driven through the hinges by the motion of a single piston (Fig. 2) at constant velocity. For the required physiological pressure drop of 100 mmHg, a flow rate of 0.555 L/min (equivalent physiological scale) is required, following the test condition previously described by Klusak *et al.*²⁶ The leakage flow rate is determined from piston velocity and area. The scale-up approach has been described and analysed in detail in previous work.^{4,26} A total measurement time of 73 ms is captured, which is only a fraction of the full leakage flow phase. Previous experimental haemodynamic performance evaluation of a clinically available 27-mm SJM BMHV²⁹ found a closure time of less than 100 ms, followed by 430 ms of leakage flow, in which the flow rate is approximately steady. In the work presented in this manuscript, the leaflets are modelled in a fixed position with leakage flow driven by constant pressure gradient. This is representative of conditions in most of the leakage flow phase, after the transient effects due to leaflet closure.

Measurement Technique

The classical 2D2C Particle Image Velocimetry (PIV) was used to measure the flow inside the scaled-up BMHV hinges model. As a source of light a dual solid-state Neodymium:Yttrium-Aluminium-Garnet

(Nd:YAG) laser (PIV Gemini Y100-15, TSI Inc.) was used. A CCD camera with 2048×2048 $7.4 \mu\text{m} \times 7.4 \mu\text{m}$ pixels (model: 630159 POWERVIEW™ Plus 4MP, TSI Inc.), was utilised to capture images of particles in flow. A 105 mm $f/2.8$ Sigma EX DG OS HSM Macro lens was used at $f/5.6$ to measure the flow fields. The fluid was seeded with silver coated glass particles, with $14 \mu\text{m}$ particle diameter and a mass density of 1100 kg/m^3 (10089-SLVR, TSI Inc., USA).

To measure the flow fields the laser pulse separation time Δt was set to $1500 \mu\text{s}$ for measurements inside the hinge, and Δt of $1000 \mu\text{s}$ for measurement inside the hinge below the leaflet, with a pulse rate of 7.25 Hz in all cases. A series of 250 images, giving a total measurement time of 73 ms (in physiological scale), was acquired for each operating condition.

Images were pre-processed with a Gaussian low-pass filter prior to image correlation to ensure all seed particle images were 3-5 pixels in diameter. Images inside the hinge, acquired at planes -86 to $-430 \mu\text{m}$, and at $-516 \mu\text{m}$, were processed with a 32×32 interrogation window size with 50% window overlap, resulting in effective measurement region of $64.6 \mu\text{m}$ and a vector spacing of $32.3 \mu\text{m}$ in the measurement ($x-y$) plane. Images inside the hinge, located between the hinge base and the leaflet protrusion (planes -588 and $-502 \mu\text{m}$), were processed with a 64×64 interrogation window size with 50% window overlap, resulting in an effective measurement region of $137 \mu\text{m}$ and a vector spacing of $68.5 \mu\text{m}$ in the measurement ($x-y$) plane. At these conditions, correlation error is estimated using published methods^{33,34} at approximately 0.05 pixels, equivalent to 0.07 m/s at physiological scale, or 1.4% of maximum velocity. Consequent uncertainty in shear stress is approximately 3.5 Pa, or 2.1% of the maximum observed.

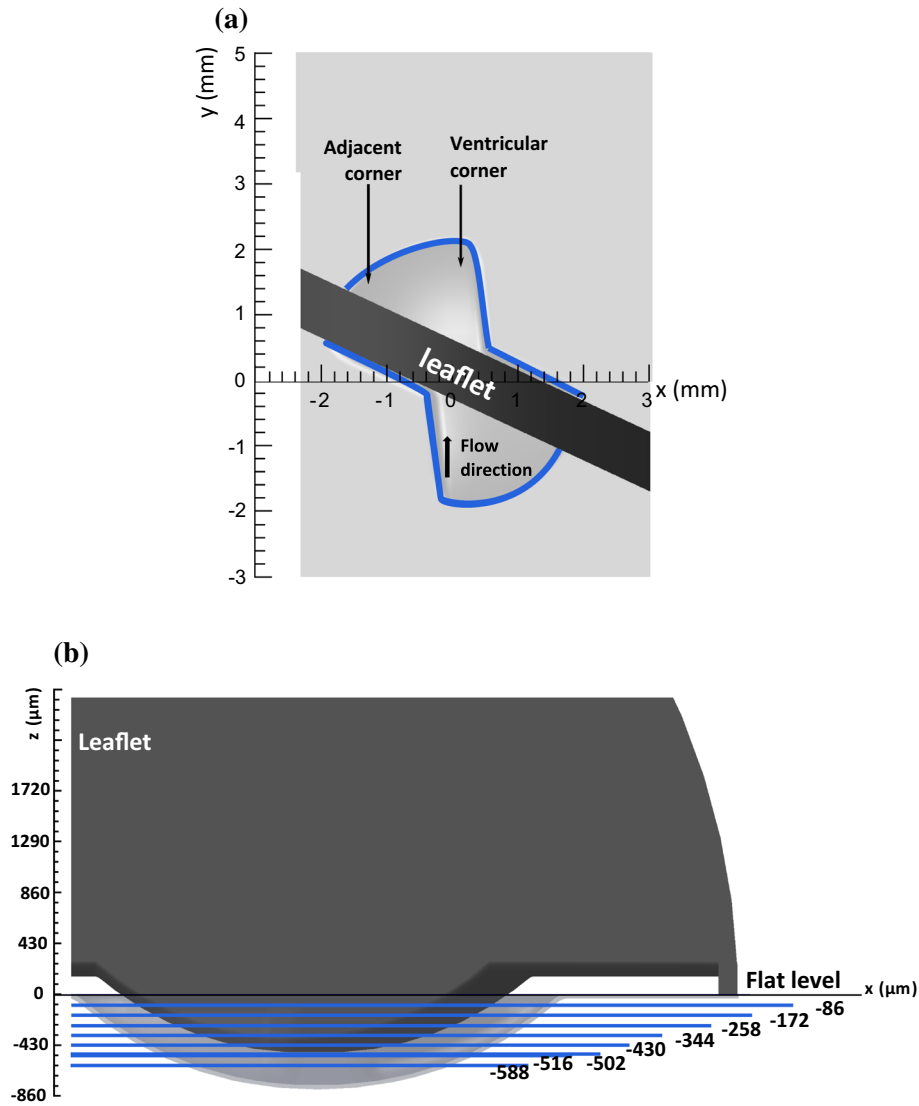


FIGURE 3. Measurement locations.

In post-processing, local validation with a median test (5×5 neighbourhood size) was applied, resulting in identification and removal of approximately 3% of measured vectors. Velocity and shear stress maps were plotted using Tecplot software (Tecplot Inc., Bellevue, WA, USA).

Time-average velocity magnitude \bar{u} was calculated using

$$|\mathbf{u}| = \frac{\sum_i \sqrt{u_i^2 + v_i^2}}{n}, \quad (2)$$

where u_i and v_i are Cartesian velocity components at measurement i , and n is the number of measurements. Time-average absolute viscous shear stresses $\bar{\tau}$ was calculated using

$$|\bar{\tau}| = \mu(\partial\bar{u}\partial y + \partial\bar{v}\partial x), \quad (3)$$

with averaged velocity gradients approximated by a central differencing scheme.

RESULTS

Time-Average Flow Field

Time-average velocity fields measured at eight elevations below the flat level are presented in Fig. 4. At planes -588 and -502 μm , located between the hinge base and the leaflet protrusion, a region of high velocity (up to 5.5 m/s) can be observed, as shown in Figs. 4g and 4h. At elevations closer to the flat level, between planes at -344 and -86 μm , two high-velocity regions are present in the adjacent and ventricular corners, formed by the leakage flow flowing

around the leaflet protrusion. A Reynolds number of 215 has been found, based on maximum velocity of 5 m/s, gap width of 150 μm and dynamic viscosity of 3.5 cP.

The time-average viscous shear stress fields measured inside the hinge are shown in Fig. 5. The highest stresses measured inside the hinge ranges up to 140 Pa. At planes -588 and -502 μm , high shear stress regions appear near the adjacent corner of the hinge. From plane -516 to -172 μm , high shear stress regions originate near the ventricular corner, whereas at plane -86 μm , the high shear stress region is found near the adjacent corner.

To quantify unsteadiness in the flow, the root mean square (rms) velocity fluctuation, expressed as a percentage of global maximum average velocity, are shown in Fig. 6. The rms velocity ranges up to 29% of maximum averaged velocity. The highest velocity rms are located near the ventricular corner. At -588 and -502 μm (Figs. 6d and 6e), low velocity flow with rms velocity between 0 and 5 % is observed in the center of the hinge cavity. However, a high-rms band ranging between 20 and 30 % is present at both elevations, as indicated with the arrow in Figs. 6d and 6e.

Instantaneous Flow Field

Instantaneous flow fields for arbitrarily selected times $t_1 = 29$ ms and $t_2 = 58$ ms, for three representative planes, are shown in Fig. 7.

At plane -86 μm , a high velocity region in the adjacent and ventricular corners is evident in Figs. 7a and 7d. The maximum velocity, up to 5.56 m/s, was measured at $t_1 = 29$ ms. The structure of the flow field at this plane appears similar throughout entire measurement time.

At plane -588 μm , the high-velocity region in the centre of the hinge cavity is present with the velocity up to 5.32 m/s, measured at time $t_1 = 29$ ms. Similarly to plane -86 μm , the strong leakage jet appears at two selected time points without evident changes in the structure and magnitude. This indicated that the leakage flow, flowing between the leaflet protrusion and the hinge base, remains high in velocity magnitude, providing washout throughout diastole.

Instantaneous viscous shear stress fields for selected times $t_1 = 29$ ms and $t_2 = 58$ ms are shown in Fig. 7. The shear stress fields are highly non-uniform and unsteady, with small regions of stress up to 160 Pa and

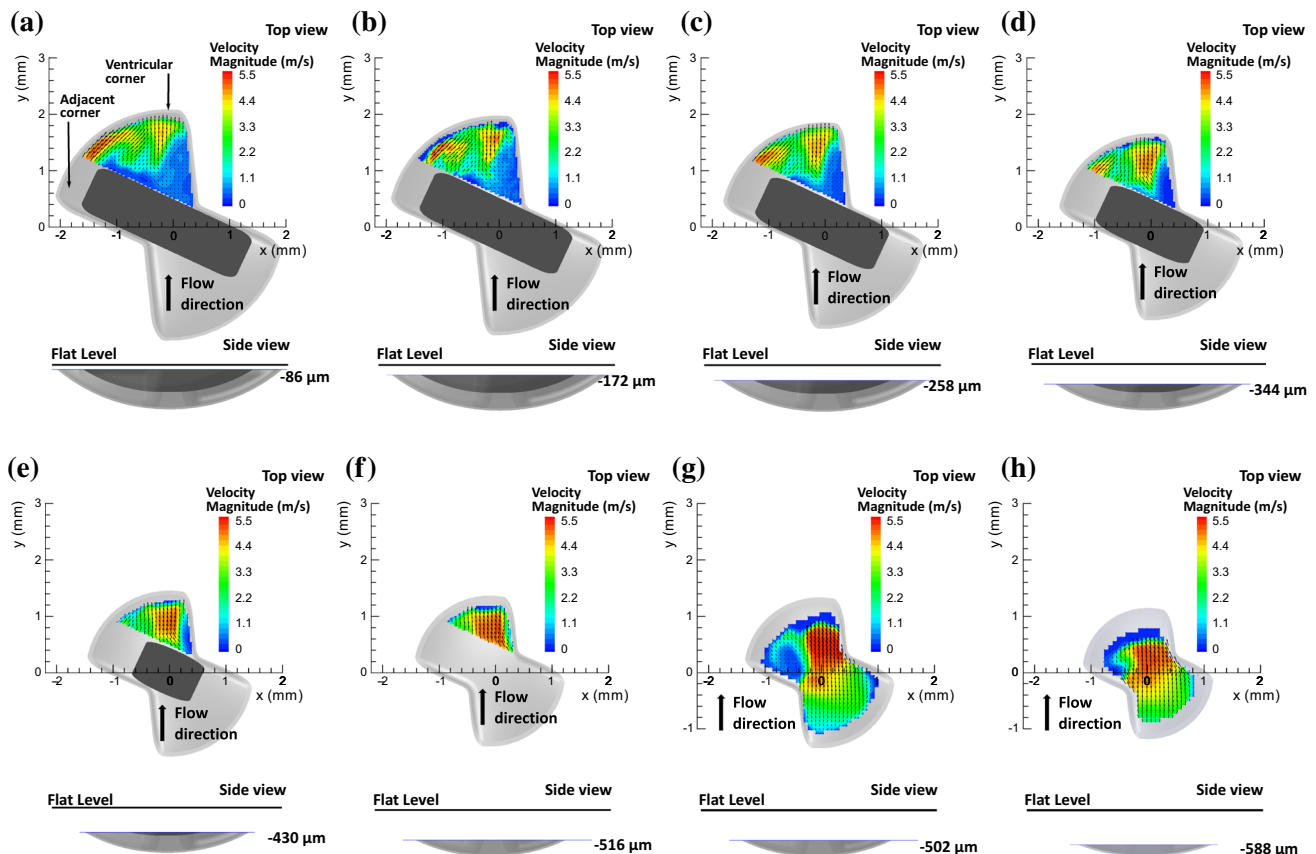


FIGURE 4. Time-average velocity contours inside the hinge, measured at eight elevations below the flat level. Results are presented in physiological scale.

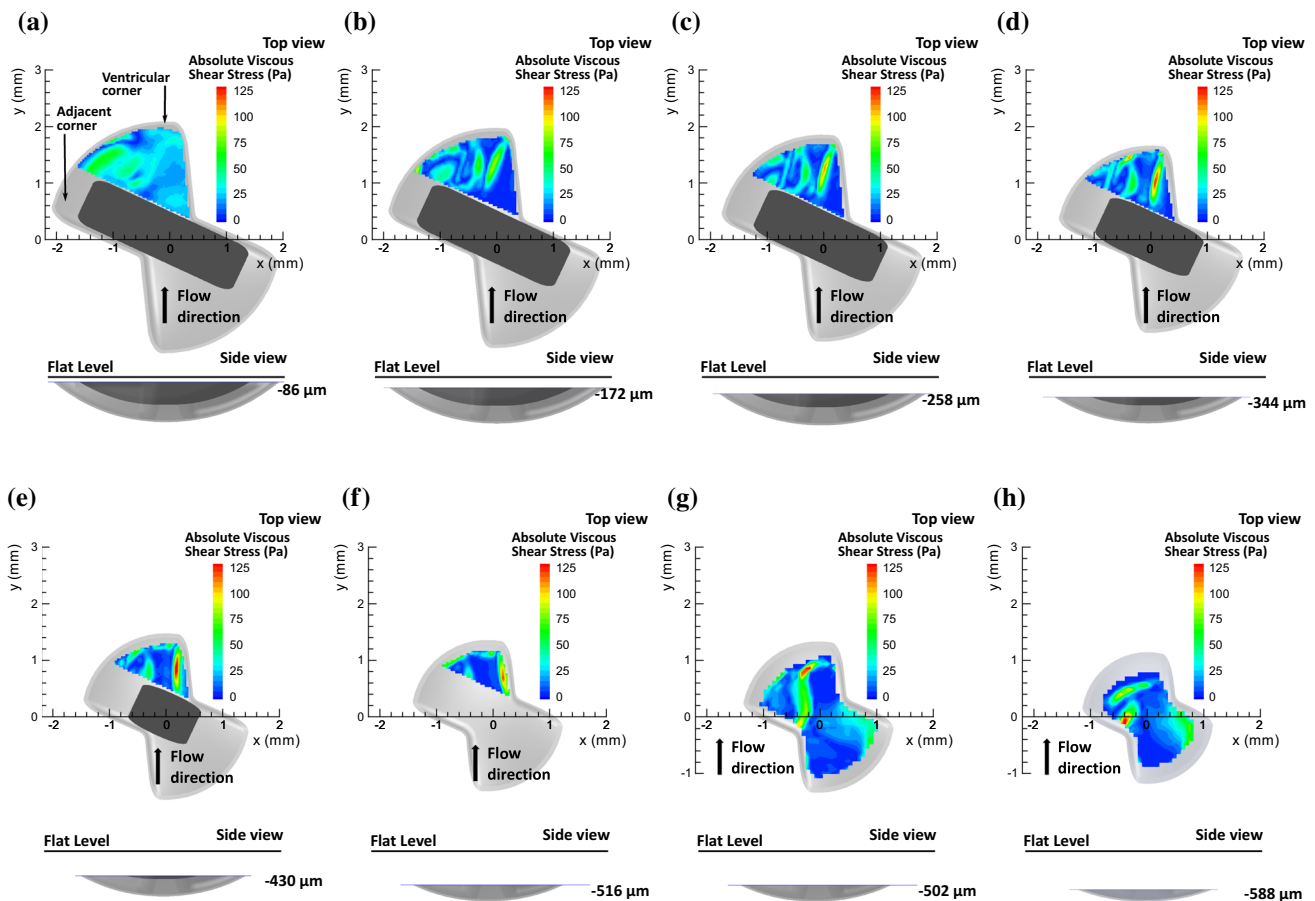


FIGURE 5. Time-average viscous shear stress contours inside the hinge, measured at eight planes below the flat level. Results are presented in physiological scale.

168 Pa, measured above and inside the hinge, respectively.

Inside the hinge cavity, the large region of elevated shear stress is present near the adjacent corner with highly non-uniform structure in the rest of the cavity.

DISCUSSION

Previous studies have suggested that the leakage flow inside hinges of a BMHV produces unsteady flow structures that have the potential for blood cell damage and initiation of coagulation processes.^{6,12,15} The objective of this study was to characterise the leakage flow inside the hinge of a BMHV, in order to gain insight into its role in blood damage. Flow fields were measured inside the hinge at eight elevations below the flat level. For the first time, whole-field time-resolved measurements of velocity fields were taken inside the hinge. Furthermore, these measurements were conducted with finer out-of-plane spatial resolution (86 μm) and deeper inside the cavity (down to 588 μm below the flat) than any previous experiments.

Comparison with Previous Results

Velocity Fields

The three-dimensional nature of the leakage flow was evident in this study. This was previously shown in numerical and experimental studies of the flow inside BMHV hinges by Simon *et al.*³⁷ and Jun *et al.*²³ The instantaneous velocity fields and rms velocity fluctuations up to 30 % indicate that the leakage flow inside the hinge is highly unsteady. Velocity ranges from 4.50 to 5.66 m/s (Fig. 4), which is consistent with computational results of Simon *et al.*,^{36,37} where velocity magnitude between 4.75 and 5.25 m/s was measured. (Previously measured velocity and viscous shear stress in and downstream of the hinges of SJM BMHVs have been summarized by Klusak *et al.*²⁶)

However, velocity magnitude measured inside the hinge is higher than previously reported in *in vitro* $\mu\text{-PIV}$ study experiments by Jun *et al.*,²³ where the global maximum velocity measured was 3.27 m/s, observed inside the hinge on plane $z = -390 \mu\text{m}$. The discrepancy between velocity magnitudes reported in this work and in the $\mu\text{-PIV}$ study of Jun *et al.*²³ may result

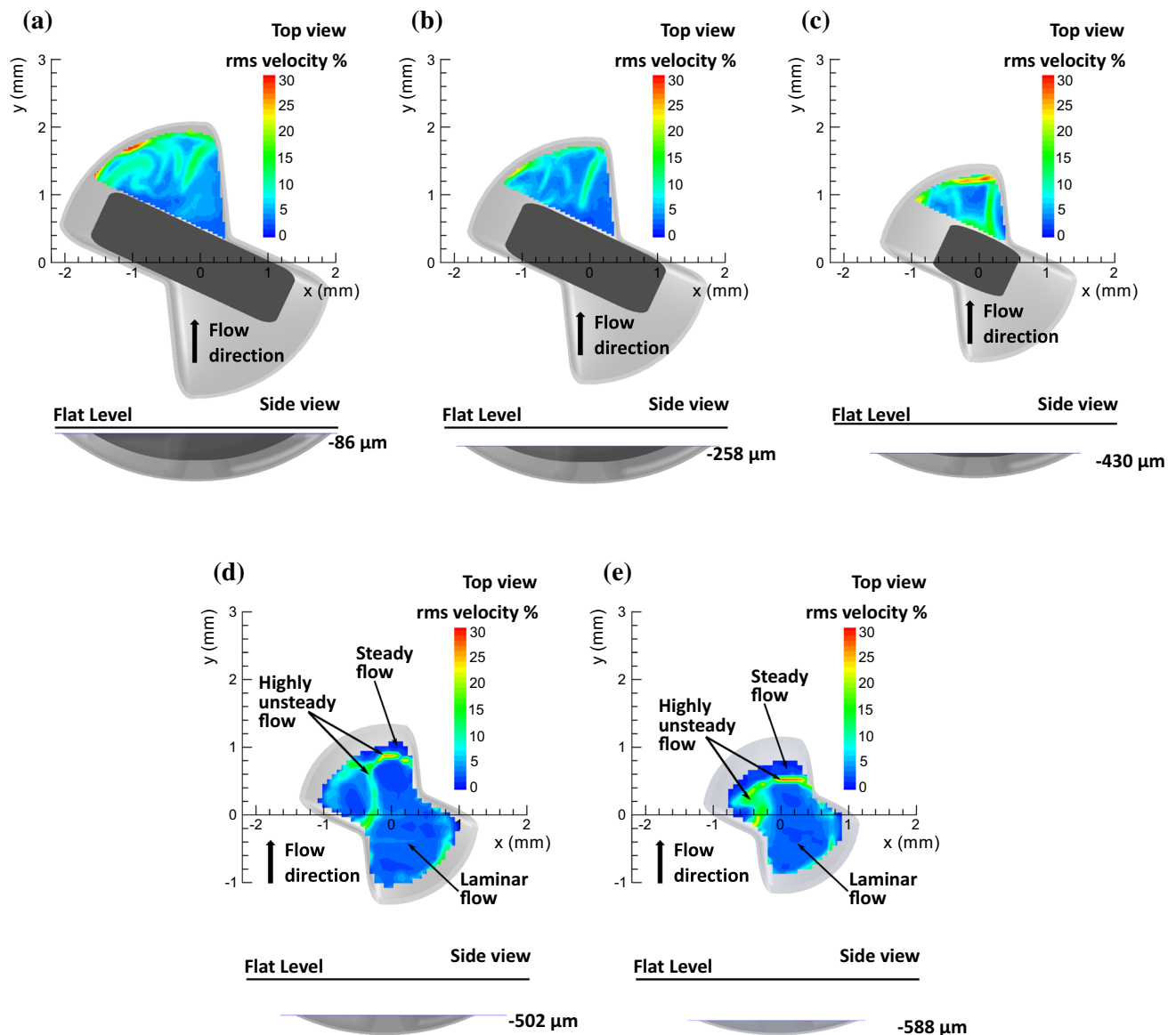


FIGURE 6. Root mean square (rms) velocity fluctuation inside the hinge cavity.

from various factors. First, the measurement principles of standard 2D2C PIV and μ -PIV differ. In standard 2D2C PIV, the effective thickness of the measurement plane is determined by the thickness of the laser light sheet, which in the present study is $86 \mu\text{m}$ (in equivalent physiological scale). In the μ -PIV study of Jun *et al.*²³ the effective thickness of measurement plane is determined by the depth of field of the microscope objective, and was between 120 and $317.4 \mu\text{m}$. Hence, the resulting measurement thickness is greater and flow fields are averaged over a thicker plane than in the present work.

As shown in the present study, where six planes inside the hinge cavity were captured, the variation of the velocity with elevation below the hinge base (i.e. z)

is significant. Thus, averaging over a greater measurement volume could affect the results. This can be demonstrated, for example, by averaging velocity measured at $x = 0 \text{ mm}$, $y = 0.5 \text{ mm}$ in the present work. The velocity on three measurement planes at $z = -516 \mu\text{m}$, $z = -430 \mu\text{m}$ and $z = -344 \mu\text{m}$ is approximately 4.5, 3.5 and 1.1 m/s, respectively (Fig. 4). The average velocity at this location over three consecutive planes, representing approximately $172 \mu\text{m}$ effective thickness of measurement volume, is 3.0 m/s, at transvalvular pressure of 100 mmHg. This results in 33 % drop of apparent velocity magnitude. In the data of Jun *et al.*,²³ at approximately equivalent (x, y) location and $-390 \mu\text{m}$ in hinge, the measured velocity ranges from 2.68 to 3.24 m/s at transvalvular

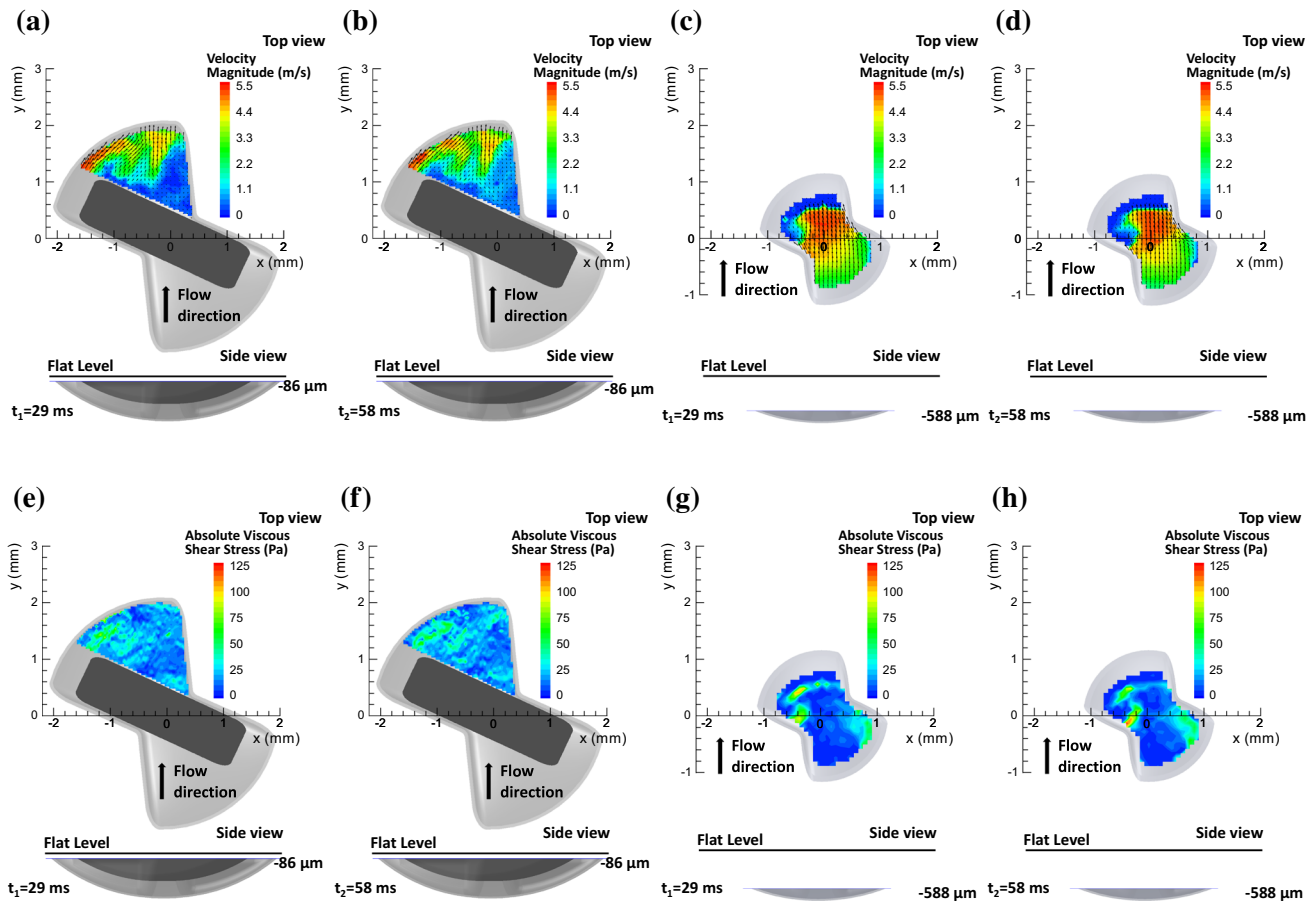


FIGURE 7. Instantaneous flow fields inside the hinge, measured at $-86 \mu\text{m}$ and at $-588 \mu\text{m}$ below flat level. Results are presented in physiological scale.

pressure of 80 and 120 mmHg, respectively. This is consistent with the value of 3.0 m/s obtained by spatial averaging in the present work, and is evidence that differences between previous and present work are due to high resolution.

Other factors that may contribute to overall differences between output results in the present study and that of Jun *et al.*²³ are differences in the BMHV models. Jun *et al.*²³ utilised a replica of a clinically available SJM BMHV valve, where leaflets are not constrained in rotation or in transverse motion along their axis. In the present work, a constant gap width of $150 \mu\text{m}$ is imposed, with the leaflet in a fixed position.

μ -CT analysis of hinge regions of a SJM BMHV, conducted in this study, showed that there is hinge gap width variation in a clinically available model. Variation in hinge gap geometry may impact the direction and velocity magnitude of leakage flow. In previous work,²⁶ we found that velocity of leakage jets downstream (on the ventricular side of) the hinge increased by 12% when gap width increased from 150 to $250 \mu\text{m}$. A similar trend was observed in a computational study

by Simon *et al.*³⁶ As the as-installed gap width was not reported in the experiments of Jun *et al.*,²³ it is possible that gap width is another contributing factor to discrepancies.

Another investigation of leakage flow in the hinge of a BMHV, performed by Ellis *et al.*¹⁶ with LDV, revealed maximum velocity of 3.40 m/s at $z = -485 \mu\text{m}$. A later LDV study³⁸ reported velocity magnitudes of 2.27 m/s at $-390 \mu\text{m}$ below the flat. Both studies utilised a replica SJM BMHV model. These values are lower than in our new results, and again they may be explained by resolution effects. In both LDV studies, data were collected with an $21 \mu\text{m} \times 140 \mu\text{m}$ ellipsoidal measurement volume. The grid spacing between measurements were $130 \times 250 \mu\text{m}$ ¹⁶ and $203 \times 203 \mu\text{m}$.³⁸ At the plane closest to the hinge base, i.e. $z = -585 \mu\text{m}$, Ellis *et al.*¹⁶ conducted measurements for $n = 3$ data points, and total of $n = 30$ within entire hinge cavity at all elevations. In the present work, the size of flow features measured in the hinge ranges from 200 to $600 \mu\text{m}$ (Figs. 4 and 5). In LDV, both the measurement volume dimensions and the spacing between measurements are

on the order of the size of these flow features, suggesting that the measurements may under-resolve the field. The present, whole-field, high-resolution measurement offered by scaled-up PIV is necessary to resolve these structures.

Blood Damage

The linearised rate of incidence of thromboembolism and bleeding post MHVs implantation was estimated to be 1.9% per patient-year and 3.0% per patient-year.³⁹ Previous studies have indicated that platelets are known to be sensitised by prior exposure to high shear stress,³⁵ thus intermittent exposure to elevated shear stress may induce their damage. Although more research is needed to determine the origin of thrombus formation in mechanical heart valves, previous BMHV explants indicated that the hinge cavity may be a favourable location for thrombus attachment and growth.^{10,42} Previous blood damage experiments^{8,21,27,30,35,43} estimated the threshold of haemolysis and the critical level for platelet activation as 150 and 10 Pa, respectively. Viscous shear stress were calculated from the present velocity fields measurements, to determine the potential of blood element damage due to leakage flow through BMHV hinges. Maximum time-average τ inside the hinge ranges up to 136 Pa and instantaneous τ ranges up to 168 Pa. This findings indicate that the instantaneous shear stress does exceed the threshold of haemolysis and the critical level for platelet activation. Time-average viscous shear stress remain below the threshold of haemolysis but exceeds the critical value for platelet activation.

Flow Features

Previous studies have suggested that presence of stagnation and recirculation regions with flow separation may be favourable for platelet aggregation and thrombus lodgement.⁴⁴ Moreover, previous BMHV explants indicated that hinge cavity may be a favourable location for thrombus attachment and growth.^{10,42}

Possible flow separation from the surface of the hinge cavity has been identified. Near the ventricular (top right in plots) corner, a region of very high velocity (> 5 m/s) is immediately upstream of a region of low velocity (< 0.3 m/s), separated by a narrow band of very high velocity gradient. This suggests a line of flow separation on the hinge cavity surface, with a family of streamlines dividing the mainstream flow from low-speed recirculating flow, as depicted schematically in Fig. 9. The rms velocity fields show highly unsteady velocity in this band of high velocity gradient, with fluctuations up to 30% (Figs. 8b and 8d). This may be due to small rapid changes in the position

of the flow separation line, and might be an origin of turbulence in the leakage jet. The proposed flow separation structure inside the hinge cavity is shown schematically in Fig. 9. Flow separation has been previously identified to play a significant role in blood element damage. Elevated shear stress in the separation region exposes blood elements to increased loading, and eventually leads to damage.^{1,2,14,19}

Limitations

In this study, leaflets were modelled in a single fixed position. In reality, leaflets are free to translate along their axis of rotation, and this motion would result in hinge gap variation from cycle and perhaps dynamic variation. Furthermore, in this study leakage flow is driven by constant pressure gradient. This constant pressure gradient, and fixed leaflet position, are expected to be representative of conditions throughout most of the leakage flow phase, after the initial transient effects due to leaflet closure. However, further work is required to investigate these effects, and to study the closing transients in detail.

We have modelled blood as a Newtonian fluid. With hinge gap width (150 μm) on the order of 20 red blood cell diameters, it is likely that non-Newtonian effects are significant, and this requires further investigation.

High-resolution PIV data can enable the generation of Lagrangian particle trajectories by integrating the velocity field in time.^{5,26} However, this is valid only if flow is strongly confined to the measurement plane, for example on a symmetry plane. Present results show that the flow inside the hinge is strongly three-dimensional. Consequently it is not meaningful to track particles, as they cannot be tracked in their out-of-plane motion. In future work, this might be overcome by measuring the out-of-plane velocity component with stereoscopic or holographic PIV.

CONCLUSIONS

This study documents the first in-hinge measurements of the leakage flow through the BMHV hinge with high spatial and temporal resolution in the same experiment. Moreover, implementation of a scaled-up model enabled measurements at unmatched out-of-plane resolution, which remain challenging in PIV experiments with clinical scale BMHVs. The results highlight the three-dimensional nature of the hinge leakage flow. High shear stress was observed, with values up to 140 Pa (average) and 168 Pa (instantaneous), above the thresholds for haemolysis and platelet activation. Results align with previous high-resolution computational studies of the flow through

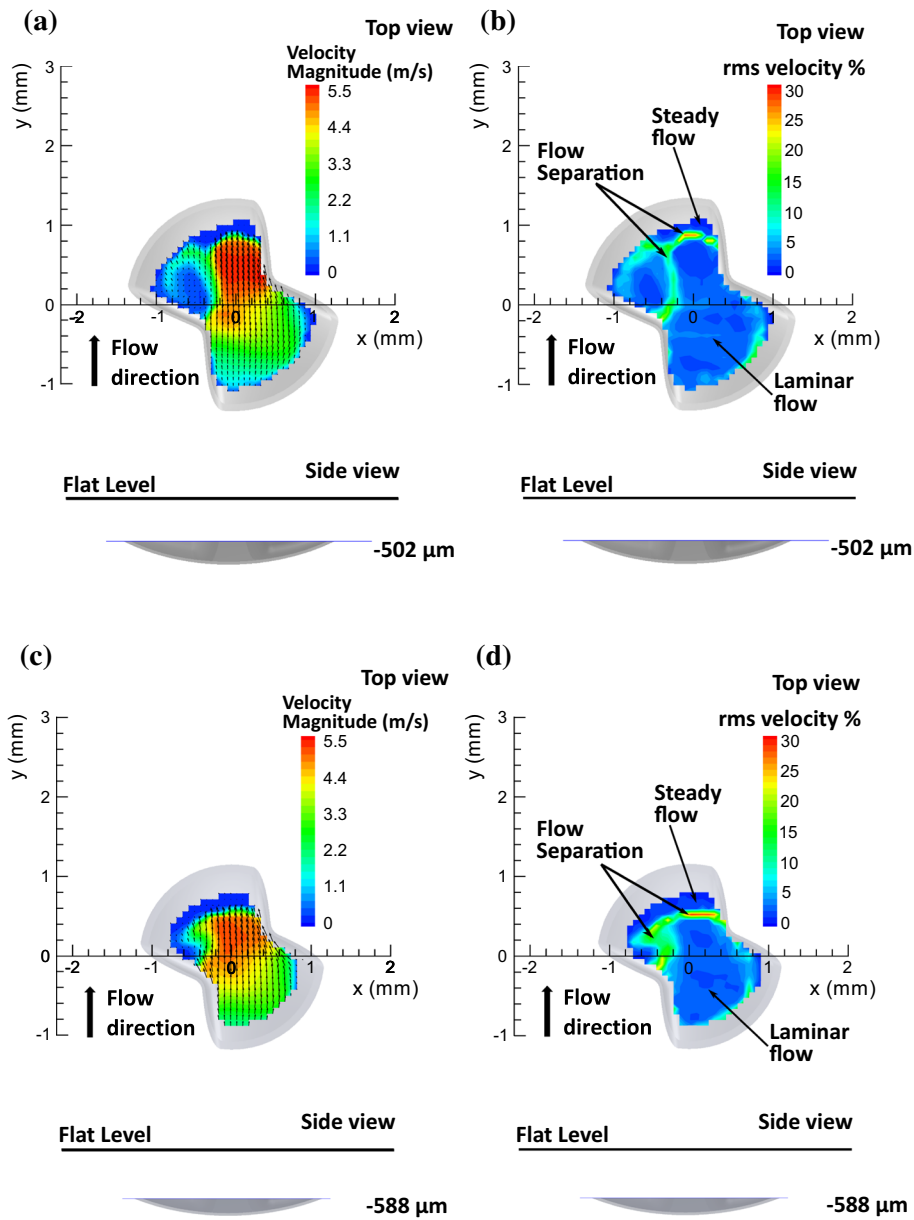


FIGURE 8. Potential flow separation inside the hinge cavity. Results are presented in physiological scale.

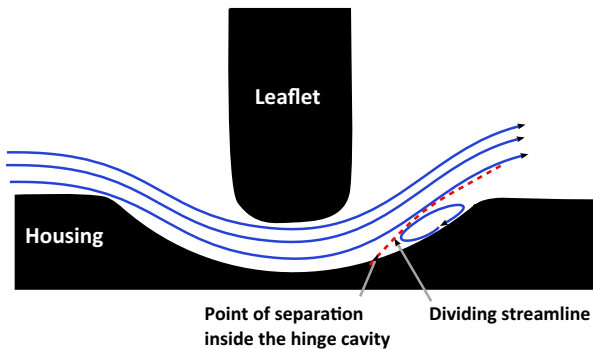


FIGURE 9. Schematic diagram of the possible flow separation inside the hinge cavity.

BMHV hinges. Discrepancies are apparent between present results and previous *in vitro* studies, but they may be explained by higher spatial resolution in the new work. Furthermore, a likely flow separation was observed in the ventricular region of the hinge for the first time. This may have thrombogenic potential, and may be a source of turbulence in the downstream leakage jets. These results provide insight into the flow features in the hinge which give rise to non-physiological shear stresses, and may guide the future development of less thrombogenic hinge designs.

ACKNOWLEDGEMENTS

The authors gratefully acknowledge the support of Science Foundation Ireland (SFI) under the Research Frontiers Programme.

FUNDING

This study was funded by Science Foundation Ireland (grant number 11/RFP.1/ENM/3310).

CONFLICT OF INTEREST

The authors declared that they have no conflict of interest.

ETHICAL APPROVAL

This article does not contain any studies with human participants or animals performed by any of the authors.

REFERENCES

- ¹Affeld, K., K. Schichl, and A. Ziemann. Flow separation in artificial heart valves. In: *Physics of Separated Flows—Numerical, Experimental, and Theoretical Aspects*, edited by K. Gersten. Wiesbaden: Springer Fachmedien Wiesbaden, 1993, pp. 184–191.
- ²Alemu, Y., and D. Bluestein. Flow-induced platelet activation and damage accumulation in a mechanical heart valve: numerical studies. *Artif. Organs* 31(9):677–688, 2007.
- ³Baber, U., S. Van der Zee, and V. Fuster. Anticoagulation for mechanical heart valves in patients with and without atrial fibrillation. *Curr. Cardiol. Rep.* 12(2):133–139, 2010.
- ⁴Bellofiore, A., E. M. Donohue, and N. J. Quinlan. Scale-up of an unsteady flow field for enhanced spatial and temporal resolution of PIV measurements: application to leaflet wake flow in a mechanical heart valve. *Exp. Fluids* 51:161–176, 2011a.
- ⁵Bellofiore, A., and N. J. Quinlan. High-resolution measurement of the unsteady velocity field to evaluate blood damage induced by a mechanical heart valve. *Ann. Biomed. Eng.* 39:2417–2429, 2011b.
- ⁶Bluestein, D., K. B. Chandran, and K. B. Manning. Towards non-thrombotic performance of blood recirculating devices. *Ann. Biomed. Eng.* 38:1236–1256, 2010.
- ⁷Brennan, J. M., F. H. Edwards, Y. Zhao, S. O'Brien, M. E. Booth, R. S. Dokholyan, P. S. Douglas, and E. D. Peterson. Long-term safety and effectiveness of mechanical versus biologic aortic valve prostheses in older patients: results from the Society of Thoracic Surgeons Adult Cardiac Surgery National Database. *Circulation* 127(16):1647–1655, 2013. <https://doi.org/10.1161/CIRCULATIONAHA.113.002003>.
- ⁸Brown C. H., L. B. Leverett, C. W. Lewis, C. P. Alfrey, and J. D. Hellums. Morphological, biochemical, and functional changes in human platelets subjected to shear stress. *J. Lab. Clin. Med.* 86(3):462–471, 1975.
- ⁹Butany, J., M. S. Ahluwalia, C. Munroe, C. Fayet, C. Ahn, P. Blit, C. Kepron, R. J. Cusimano, and R. L. Leask. Mechanical heart valve prostheses: identification and evaluation (erratum). *Cardiovasc. Pathol.* 12(6):322–344, 2003.
- ¹⁰Butchart, E. G. Antithrombotic management in patients with prosthetic valves: a comparison of American and European guidelines. *Heart* 95(5):430–436, 2009. <https://doi.org/10.1136/hrt.2007.134726>.
- ¹¹Cannegieter, S. C., F.R. Rosendaal, and E. Briet. Thromboembolic and bleeding complications in patients with mechanical heart valve prostheses. *Circulation* 89(2):635–641, 1994. <https://doi.org/10.1161/01.CIR.89.2.635>.
- ¹²Chandran, K. B. Dynamics behavior analysis of mechanical heart valves prostheses. In: *Biomechanical Systems: Techniques and Applications, Vol. II: Cardiovascular Techniques II:3-6–3-29*. Boca Raton: CRC Press, 2000.
- ¹³DeWall, R. A., N. Qasim, and L. Carr. Evolution of mechanical heart valves. *Ann. Thorac. Surg.* 69(5):1612–1621, 2000.
- ¹⁴Ellis, J. T. An in vitro investigation of the leakage and hinge flow fields through bileaflet mechanical heart valves and their relevance to thrombogenesis. Dissertation, Georgia Institute of Technology, 1999.
- ¹⁵Ellis, J. T., T. M. Healy, A. A. Fontaine, R. Saxena, and A.P. Yoganathan. Velocity measurements and flow patterns within the hinge region of a Medtronic Parallel bileaflet mechanical valve with clear housing. *J. Heart Valve Dis.* 5:591–599, 1996.
- ¹⁶Ellis, J. T., B. R. Travis, and A. P. Yoganathan. An in vitro study of the hinge and near-field forward flow dynamics of the St. Jude Medical Regent bileaflet mechanical heart valve. *Ann. Biomed. Eng.* 28:524–532, 2000.
- ¹⁷Fallon, A. M., N. Shah, U. M. Marzec, J. N. Warnock, A. P. Yoganathan, and S. R. Hanson. Flow and thrombosis at orifices simulating mechanical heart valve leakage regions. *J. Biomech. Eng.* 128(1):30, 2006. <https://doi.org/10.1115/1.2133768>.
- ¹⁸Gott, V. L., D. E. Alejo, and D. E. Cameron. Mechanical heart valves: 50 years of evolution. *Ann. Thorac. Surg.* 76(6):S2230–S2239, 2003. <https://doi.org/10.1016/j.athoracur.2003.09.002>.
- ¹⁹Govindarajan, V., H. S. Udaykumar, L. H. Herbertson, S. Deutsch, K. B. Manning, and K. B. Chandran. Impact of design parameters on bileaflet mechanical heart valve flow dynamics. *J. Heart Valve Dis.* 18(5):535–545, 2009. <http://www.scopus.com/inward/record.url?eid=2-s2.0-77449122865&partnerID=40&md5=a6a976c71a80a9b4d0c4f8697bd80476>.
- ²⁰Hammermeister, K., G. K. Sethi, W. G. Henderson, F. L. Grover, C. Oprian, and S. H. Rahimtoola. Outcomes 15 years after valve replacement with a mechanical versus a bioprosthetic valve: final report of the veterans affairs randomized trial. *J. Am. Coll. Cardiol.* 36(4):1152–1158, 2000.
- ²¹Hellums, J., D. Peterson, N. Stathopoulos, J. Moake, and T. Giorgio. Studies on the mechanisms of shear-induced platelet activation. In: *Cerebral Ischemia and Hemorheology*, edited by A. Hartmann and W. Kuschinsky. Berlin: Springer, 1987, pp. 80–89.

- ²²Herbertson, L. H., S. Deutsch, and K. B. Manning. Near valve flows and potential blood damage during closure of a bileaflet mechanical heart valve. *J. Biomech. Eng.* 133:094507, 2011.
- ²³Jun, B. H., N. Saikrishnan, and A. P. Yoganathan. Micro particle image velocimetry measurements of steady diastolic leakage flow in the hinge of a St. Jude medical regent mechanical heart valve. *Ann. Biomed. Eng.* 42:526–540, 2014.
- ²⁴Kameneva, M. V., G. W. Burgreen, K. Kono, B. Repko, J. F. Antaki, and M. Umezu. *Effects of turbulent stresses upon mechanical hemolysis: experimental and computational analysis.* *ASAIO J.* 50(5):418–423, 2004.
- ²⁵Kaneko, T., and S. F. Aranki. Anticoagulation for prosthetic valves. *Thrombosis* 2013:346752, 2013.
- ²⁶Klusak, E., A. Bellofiore, S. Loughnane, and N. J. Quinlan. High-resolution measurements of velocity and shear stress in leakage jets from bileaflet mechanical heart valve hinge models. *J. Biomech. Eng.* 137(11):111008, 2015.
- ²⁷Leverett, L. B., J. D. Hellums, C. P. Alfrey, and E. C. Lynch. Red blood cell damage by shear stress. *Biophys. J.* 12:257–273, 1972.
- ²⁸Manning, K. B., V. Kini, A. A. Fontaine, S. Deutsch, and J. M. Tarbell. Regurgitant flow field characteristics of the St. Jude bileaflet mechanical heart valve under physiologic pulsatile flow using particle image velocimetry. *Artif. Organs* 27:840–846, 2003.
- ²⁹Nobili, M., U. Morbiducci, R. Ponzini, C. Del Gaudio, A. Balducci, M. Grigioni, F. M. Montevecchi, and A. Redaelli. Numerical simulation of the dynamics of a bileaflet prosthetic heart valve using a fluidstructure interaction approach. *J. Biomech.* 41:2539–2550, 2008.
- ³⁰Paul, R., J. Apel, S. Klaus, F. Schügner, P. Schwindke, and H. Reul. Shear stress related blood damage in laminar couette flow. *Artif. Organs* 27:517–529, 2003.
- ³¹Pibarot, P., and J. G. Dumesnil. Prosthetic heart valves: selection of the optimal prosthesis and long-term management. *Circulation* 119(7):1034–1048, 2009.
- ³²Quinlan, N. J., and P. N. Dooley. Models of flow-induced loading on blood cells in laminar and turbulent flow, with application to cardiovascular device flow. *Ann. Biomed. Eng.* 35(8):1347–1356, 2007. <https://doi.org/10.1007/s10439-007-9308-8>.
- ³³Raffel, M., C. Willert, S. Wereley, and J. Kompenhans. *Particle Image Velocimetry: A Practical Guide.* Berlin: Springer, 2007.
- ³⁴Raghav, V., S. Sastry, and N. Saikrishnan. Experimental assessment of flow fields associated with heart valve prostheses using particle image velocimetry (PIV): recommendations for best practices. *Cardiovasc. Eng. Technol.* 9:273–287, 2018.
- ³⁵Sheriff, J., D. Bluestein, G. Girdhar, and J. Jesty. High-shear stress sensitizes platelets to subsequent low-shear conditions. *Ann. Biomed. Eng.* 38:1442–1450, 2010.
- ³⁶Simon, H. A., L. Ge, I. Borazjani, F. Sotiropoulos, and A. P. Yoganathan. Simulation of the three-dimensional hinge flow fields of a bileaflet mechanical heart valve under aortic conditions. *Ann. Biomed. Eng.* 38:841–853, 2010a.
- ³⁷Simon, H. A., L. Ge, F. Sotiropoulos, and A. P. Yoganathan. Numerical investigation of the performance of three hinge designs of bileaflet mechanical heart valves. *Ann. Biomed. Eng.* 38:3295–3310, 2010b.
- ³⁸Simon, H. A., H. L. Leo, J. Carberry, and A. P. Yoganathan. Comparison of the hinge flow fields of two bileaflet mechanical heart valves under aortic and mitral conditions. *Ann. Biomed. Eng.* 32:1607–1617, 2004.
- ³⁹Toole, J. M., M. R. Stroud, J. M. Kratz, A. J. Crumbley, S. M. Bradley, F. A. Crawford, and J. S. Ikonomidis. Twenty-five year experience with the St. Jude medical mechanical valve prosthesis. *Ann. Thorac. Surg.* 89(5):1402–1409, 2010. <https://doi.org/10.1016/j.athoracsur.2010.01.045>.
- ⁴⁰Travis, B. R., H. L. Leo, P. A. Shah, D. H. Frakes, and A. P. Yoganathan. An analysis of turbulent shear stresses in leakage flow through a bileaflet mechanical prostheses. *J. Biomech. Eng.* 124:155, 2002.
- ⁴¹Vallana, F., S. Rinaldi, P. Galletti, A. Nguyen, and A. Piwnica. Pivot design in bileaflet valves. *ASAIO J.* 38:M600–M606, 1992.
- ⁴²Wilke, A., C. M. Wende, M. Horst, and D. Steverding. Thrombosis of a prosthetic mitral valve after withdrawal of phenprocoumon therapy. *Cardiol. Res.* 2(6):298–300, 2011.
- ⁴³Williams, A. R., D. E. Hughes, and W. L. Nyborg. Hemolysis near a transversely oscillating wire. *Science* 169:871–873, 1970.
- ⁴⁴Woo, Y. R., and A. P. Yoganathan. In vitro pulsatile flow velocity and shear stress measurements in the vicinity of mechanical mitral heart valve prostheses. *J. Biomech.* 19:39–51, 1986.
- ⁴⁵Yoganathan, A. P., K. B. Chandran, and F. Sotiropoulos. Flow in prosthetic heart valves: state-of-the-art and future directions. *Ann. Biomed. Eng.* 33(12):1689–1694, 2005. <https://doi.org/10.1007/s10439-005-8759-z>.
- ⁴⁶Yoganathan, A. P., Z. He, and C. S. Jones. Fluid mechanics of heart valves. *Ann. Biomed. Eng.* 6:331–362, 2004.
- ⁴⁷Yun, B. M., J. Wu, H. A. Simon, S. Arjunon, F. Sotiropoulos, C. K. Aidun, and A. P. Yoganathan. A numerical investigation of blood damage in the hinge area of aortic bileaflet mechanical heart valves during the leakage phase. *Ann. Biomed. Eng.* 40(7):1468–1485, 2012.
- ⁴⁸Zhao, J. B., Y. B. Shi, T. J. Yeo, and N. H. Hwang. Digital particle image velocimetry investigation of the pulsating flow around a simplified 2-D model of a bileaflet heart valve. *J Heart Valve Dis* 10:239–253, 2001.
- ⁴⁹Zilla, P., J. Brink, P. Human, and D. Bezuidenhout. Prosthetic heart valves: catering for the few. *Biomaterials* 29(4):385–406, 2008. <https://doi.org/10.1016/j.biomaterials.2007.09.033>.

Publisher's Note Springer Nature remains neutral with regard to jurisdictional claims in published maps and institutional affiliations.